International Journal of Bioelectromagnetism
Vol. 14, No. 1, pp. 29-33, 2012

On the accuracy of collocation and Galerkin BEM in the EEG/MEG forward problem

Matti Stenroos[a], Jukka Nenonen[b]
[a]*Dept. Biomedical Engineering and Computational Science, Aalto University, Espoo, FINLAND*
[b]*Elekta Oy, Helsinki, FINLAND*

Correspondence: M. Stenroos, P.O. Box 12440, FI-00076 Aalto, FINLAND
E-mail: matti.stenroos@tkk.fi, phone +358 50 344 3410, fax +358 9 470 23182

Abstract. In electro- and magnetoencephalography (EEG, MEG), source imaging aims to characterize, which regions of the brain give rise to the measured signals. The localization accuracy depends on the methods used in source imaging. To enable accurate localization of the source, the forward problem—the relationship between modeled sources and resulting signals—needs to be properly solved. In this work, we compare the performances of different boundary element methods (BEM) and mesh resolutions in the forward EEG/MEG problem in a realistically-shaped head model. We also present a computationally light simplification to the Galerkin BEM.

A 3-layer head model was triangulated with four mesh resolutions. Electric potential and magnetic field due to a set of dipolar sources was computed in 128 electrode and 304 magnetometer positions. The reference computations were done with a dense mesh and Symmetric BEM, and the test computations in three less dense meshes with linear Galerkin (LG), the simplified Galerkin (LGQ), and linear collocation (LC) BEMs.

The results show that, of the tested methods, the LG is the most accurate and stable one. The LGQ performs clearly better than the LC. The results suggest that the LGQ method may be a good compromise between the accuracy and computational cost.

Keywords: electroencephalography, magnetoencephalography, forward problem, inverse problem, boundary element method

1 Introduction

In electro- and magnetoencephalography (EEG, MEG), the electrical activity of the brain is studied non-invasively by measuring voltages on the scalp (EEG) and magnetic fields outside the head (MEG). Source imaging aims to characterize, which regions of the brain give rise to the measured signals. The sensitivity of EEG and MEG to brain activity depends physically on the position, orientation, and extent of the sources. The localization accuracy depends, however, also on the methods used in source imaging.

The source-imaging problem is solved in two steps. First, the anatomy (and conductivity profile) of the head is modeled with the help of anatomical magnetic resonance imaging (MRI) and image processing, and the relation between a source model and the resulting signals is solved. This is called the forward problem. Then, the source locations and strengths are estimated from the measured signals with the help of the forward solution. This part is called the inverse problem. An appropriate solution to the forward problem is an essential prerequisite for the solution of the inverse problem: the physics of the problem is in the forward model, and errors caused by an insufficient forward model cannot be corrected later.

In the first part of forward modeling, the anatomical volume conductor model is constructed: regions of different conductivities are segmented, and the segmented data are co-registered with sensor coordinates obtained during the EEG/MEG measurement. The head, as a conductor, can be assumed to consist of scalp, skull, cerebrospinal fluid (CSF), gray brain matter, and white brain matter.

The forward EEG/MEG problem is formulated with quasi-static electromagnetic theory and solved with numerical field computation in the volume conductor model. In experimental work, piece-wise homogeneous conductor models and the boundary element method (BEM) are a common and an efficient choice. An EEG volume-conductor model comprises typically the scalp, skull, and the brain regions (3-layer model). In MEG modeling, the standard approach in experimental studies has been to use a spherical model or a single-shell model that contains only the inner surface of the skull. Although the effects of model errors and simplifications are smaller for MEG than for EEG, a more correct anatomical model, such as the 3-layer model, is expected to improve the localization accuracy also in MEG.

In this work, we compare the performances of different BEM approaches and mesh resolutions in the forward EEG/MEG problem in a realistically-shaped 3-layer head model.

2 Boundary Element Method

Solving of a volume conductor problem for electric potential with the BEM consists of the following steps [Stenroos *et al.* 2007]:

- The Poisson equation is first converted to surface integral form.
- Boundary surfaces of the conductivity model are tessellated into triangle meshes.
- Potential on all conductivity boundaries is approximated with a linear combination of basis functions, defined according to the meshes (typically linearly varying potential).
- The residual of the approximated solution is minimized with respect to a set of weight functions, also defined on the meshes.
- The resulting set of algebraic equations is solved after specifying the zero-level of the potential.

The result is a linear mapping that gives boundary potentials in all discretization points Φ, given the weighted infinite-medium potentials Φ_∞:

$$\Phi = T_\Phi \Phi_\infty \,. \tag{1}$$

After solving for Φ, the magnetic field B is obtained by adding the infinite-volume fields and the fields due to the volume currents; in discretized form,

$$\mathrm{B} = \mathrm{B}_\infty + T_\mathrm{B} \Phi \,. \tag{2}$$

There are two common ways for specifying the weight functions in BEM. In collocation BEM [*e.g.*, Stenroos *et al*. 2007], the residual is point-wise minimized in all discretization points. In Galerkin BEM [Mosher *et al*. 1999, Stenroos and Haueisen 2008], the integral of the error is minimized, using the same functions as basis and weight functions. With some extra effort, the boundary-element solution can also be formulated in another fashion, solving for both surface potentials and their normal derivatives. This combined approach with integral-based residual minimization is called the Symmetric BEM [Kybic *et al*. 2005].

2.1 Error Behavior

The error in BEM solutions comes from discretization errors of the geometry and especially of the potential: if a source is too close to a boundary mesh, a low-order basis function is not able to represent the correct potential, and if two boundary surfaces are too close to each other, the boundary conditions cannot be represented properly. In addition, large conductivity-differences may pose numerical difficulties. In EEG/MEG problem, all these error sources are present: sources are close to the skull, and the skull is thin and has much lower conductivity than the surrounding tissues. A two-step BEM solution, often called “the isolated skull approach” (ISA), alleviates skull-related numerical problems [Hämäläinen and Sarvas 1989].

In simulations in spherical geometry, it has been shown that the Galerkin and Symmetric BEMs cope with these discretization problems better than the collocation BEM [Mosher *et al*. 1999, Kybic *et al*. 2005, Werner and Stenroos 2010]. Commonly used toolboxes for the analysis of EEG/MEG data (for example, Curry, BESA, MNE Suite, and the current Elekta software), however, use the collocation BEM.

2.2 Cost-effectiveness and Quick Galerkin BEM

In the construction of the T_Φ matrix, the most of the computation time goes into forming weighted double-layer integrals. The computations are carried out triangle-wise in terms of so-called shape functions (see, *e.g.*, [Stenroos *et al*. 2007]). With linear collocation BEM in a model with N vertices, approx. $6N^2$ shape-integral operations are needed. With linear Galerkin BEM, one needs to numerically integrate over the shape integrals in the field space. This gives a total of $12MN^2$ shape-integral operations, where M is the number of quadrature points per surface (typically 7 or 13). In addition, there are costs due to performing the numerical shape-function integration and due to more complicated matrix assembly. In the construction of Φ_∞, the corresponding cost-factors are N and ($2MN$ + the cost due to numerical integration and assembly). The symmetric BEM is in the construction of Φ_∞ roughly twice as costly as the Galerkin BEM.

The computational cost plays an important role in nonlinear inverse estimates where the computation of Φ_∞ is repeated hundreds of times. The cost of the Galerkin BEM can be adjusted by tuning the number of integration points, M. When M is dropped to 1, the numerical integration is considerably simplified, as numerical shape-integrals are reduced to multiplication with the triangle areas. The cost factor of Φ_∞ is then ($2N$ + a sparse-matrix multiplication that sets the integration weights). Compared to general Galerkin BEM and Symmetric BEM, the method is very straightforward to implement using any collocation BEM tools, such as the Helsinki BEM library [Stenroos *et al.* 2007]. We call this simplified Galerkin approach "Quick Galerkin BEM".

3 Model geometry

3.1 Volume conductor model

All computations were carried out in 3-layer realistically-shaped volume conductor model comprising the brain, skull, and scalp regions. The conductivities of brain and scalp were 0.33 S/m, and the conductivity of the skull 8.25 mS/m (a conductivity contrast of 40). The boundary surfaces were triangulated from a statistical head model. We used four models with same geometry but different mesh densities, comprising approximately 1000, 2000, 4000, and 10000 vertices per boundary surface, respectively. The 10000-vertex model was used as the reference; the results computed with that model were considered "accurate". The volume conductor model is displayed in Fig. 1.

3.2 Sensor geometry

The normal component of the magnetic field was computed for 304 point-magnetometer locations covering the sensor array of the Elekta Neuromag MEG system.

In EEG computations, a 128-electrode ABC electrode layout was used. The electrode template was obtained from Biosemi[1]; the template headcap was manually co-registered with rigid transformations with the 10000-vertex scalp mesh, and electrodes were projected to their nearest points on the mesh surface. The simulated potential was linearly interpolated to these electrode positions from the nodal potentials; as the potential is modeled with linear basis functions, this interpolation is a natural choice. The electrode positions of the 10000-vertex reference mesh were projected to other meshes. The MEG sensor surface and EEG electrodes are visualized in Fig. 1.

3.3 Source setup

In all simulations, a single point-like unit current dipole was used as the source. Dipoles were placed in various regions of the right hemisphere at different depths. The positions were specified as follows:

On the right hemisphere, 23 evenly-distributed reference points were chosen, roughly following a 32-electrode 10–20 layout (see Fig. 2). Around these reference positions, 8 other positions were generated at ±2 mm distances in the tangential directions. Around each of the 23 regions on the brain surface, radially and tangentially oriented unit dipoles were placed along the surface-normal at distances 2 to 40 mm from the brain surface. At each nominal depth[2], there were thus a total of 9 x 23 = 203 dipole positions. The resulting source setup is displayed in Fig. 2.

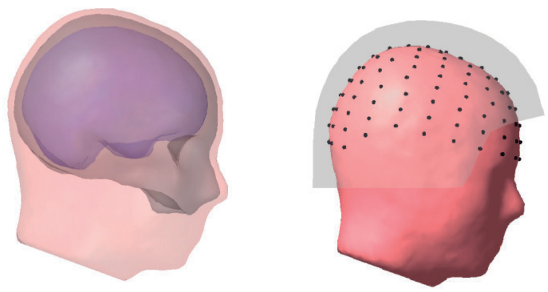

Figure 1. *The volume conductor model and sensor setup. On left, a 3-layer head model comprising the brain, skull, and scalp regions. On right, 128 EEG electrodes visualized with black dots and the MEG sensor surface visualized with transparent gray.*

[1] `http://www.biosemi.com/headcap.htm`

[2] As the head-model is not spherical, the distances along normal are not true depths; hence the term "nominal depth"

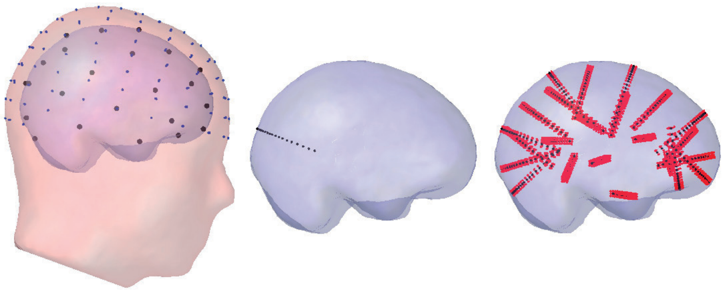

Figure 2. *The source setup. The sources are placed in 23 regions on the right hemisphere; black dots in the left plot show the centroids of these regions, and blue dots show the positions of the EEG electrodes. The source depth ranges between 2 mm and 40 mm; center plot. In each region at each depth, there are 9 source positions, placed 2 mm from each other. All source positions are shown in the rightmost plot.*

3.4 BEM implementations

The test computations were done with three BEM approaches: linear collocation BEM (LC), linear Galerkin BEM (LG), and the new quick linear Galerkin (LGQ). The reference computations were done with the Symmetric BEM [Kybic *et al*. 2005]. The LC method was modified from that presented in [Stenroos *et al*. 2007] by applying sharp-edged formulation [Stenroos 2009] that solves the so-called auto-solid angle accurately without introducing any bias to the model. The LG method was implemented as described in the appendix of [Stenroos 2009], and the symmetric BEM as described in [Kybic *et al*. 2005]. In test computations, the ISA correction was used, following the formulation in [Hämäläinen and Sarvas 1989].

4 Results

The potentials and magnetic fields resulting from the simulations were compared using the relative error measure (RE); see, *e.g.*, [Stenroos *et al.*, 2007]. The results are shown in Figs. 3 and 4. The accuracy-ranking of the methods is clear: the LG method is the most accurate, LC the least accurate, and the LGQ falls in between the LC and LG. With increasing mesh-density, the differences between the methods get smaller.

In the EEG solution, the error of LC and LGQ methods starts to increase quickly, when the distance between the source and skull is about 2/3 of the mean triangle-side-length (TSL). The LG method has smoother error behavior close to the skull. In the MEG solution, the performance of the LG and LGQ methods is very similar with deeper sources; the LC method has clearly higher overall error level. Close to the skull (less than 1 TSL), the LGQ error approaches the LC error. It is, however, important to take into account the low overall error of the MEG solution: all methods are valid, when the source is not too close to the skull.

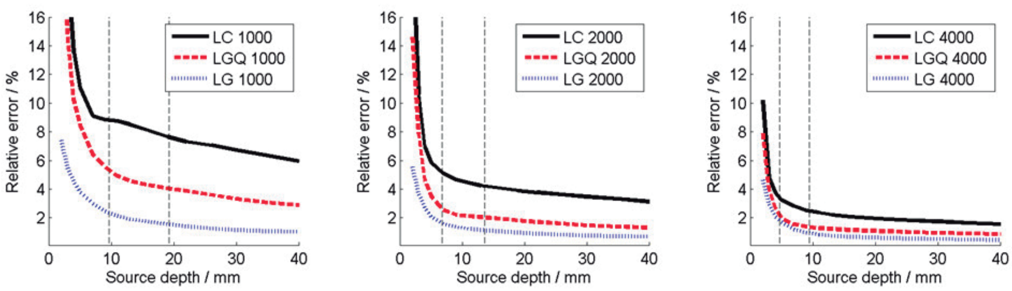

Figure 3. *Median relative error in the EEG forward solutions with normally-oriented sources; results for meshes with 1000, 2000, and 4000 vertices per surface are shown in left, middle, and rights plot, respectively. The dashed vertical lines show the depths corresponding to one and two times the mean triangle-side-length of the innermost mesh.*

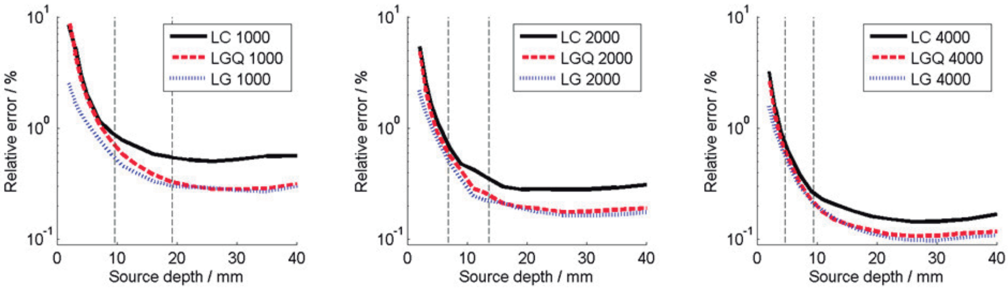

Figure 4. *Median relative error in the MEG forward solutions with tangential sources; results for meshes with 1000, 2000, and 4000 vertices per surface are shown in left, middle, and rights plot, respectively. The dashed vertical lines show the depths corresponding to one and two times the mean triangle-side-length of the innermost mesh. Notice the logarithmic scale.*

5 Discussion

In this work, we compared the performances of different boundary element methods and mesh resolutions in the forward EEG/MEG problem in a realistically-shaped 3-layer head model. Aiming at a method more accurate than LC and more cost-effective than LG, we presented a simplified Galerkin approach, called the Quick Galerkin (LGQ).

The results show the LG method is clearly the most accurate and stable of the tested methods. The LGQ method appears to perform well, too: In EEG problem, the improvement over the LC method is, in the authors' opinion, so clear that the slight increase of the computational cost is warranted. In the MEG problem, the differences are smaller.

Considering experimental use, all tested methods are likely to perform satisfactorily, if the mesh density is at least 2000 and the modeled sources are at least 7mm from the skull; at that source depth, the median error of the LC method in the EEG problem starts to grow swiftly from the 5% median error. The same median error level is with LGQ and LG methods obtained at about 4.5 mm and 2.5 mm depth, respectively.

To enable accurate amplitude-profile reconstruction for distributed inverse solutions, it is also important to consider the variance of the error. In our analysis so far, we have used the nominal depths instead of the real depths. The effects of mesh density and curvature on real source-depth may hence, in the case of superficial sources, lead to over-pessimistic figures. We thus leave the analysis of the error variance for later studies.

The LGQ method will be made available for the users of the Helsinki BEM library [Stenroos *et al*. 2007] in the near future, increasing the value of the library in EEG/MEG source imaging.

Acknowledgements

The authors wish to thank Dr. Jyrki Lötjönen for the triangle meshes and Dr. Jukka Sarvas for quadrature routines and insightful discussions.

References

Hämäläinen MS and Sarvas J. Realistic conductivity geometry model of the human head for interpretation of neuromagnetic data. *IEEE Trans Biomed Eng*, 36:165–171, 1989.

Kybic J, Clerc M, Abboud T, Faugeras O, Keriven R, Papadopoulo T. A common formalism for the integral formulations of the forward EEG problem. *IEEE Trans Med Imaging*, 24:12–28, 2005.

Mosher J, Leahy R, Lewis P. EEG and MEG: Forward solutions for inverse methods. *IEEE Transactions in Biomedical Engineering* 46: 245–259, 1999.

Stenroos M, Mäntynen V, Nenonen J. A Matlab library for solving quasi-static volume conduction problems using the boundary element method. *Computer Methods and Programs in Biomedicine*, 88:256–263, 2007.

Stenroos M, Haueisen J. Boundary element computations in the forward and inverse problem of electrocardiography: comparison of collocation and Galerkin weightings. *IEEE Transactions on Biomedical Engineering*, 55:2124–2133, 2008.

Stenroos M. The transfer matrix for epicardial potential in a piece-wise homogeneous thorax model: the boundary element formulation. *Physics in Medicine and Biology*, 54:5443–5455, 2009.

Werner P and Stenroos M.Skull thickness versus mesh density—a study on BEM discretization error. In 17th International Conference on Biomagnetics: Advances in Biomagnetism—Biomag 2010, IFMBE Proceedings,28:117–119, 2010.